Assiut University Journal of Multidisciplinary Scientific Research (AUNJMSR)
Faculty of Science, Assiut University, Assiut, Egypt.
Printed ISSN 2812-5029
Online ISSN 2812-5037
Vol. 52(3): 249- 271 (2023)
https://aunj.journals.ekb.eg

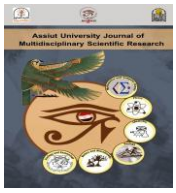

Elastic Scattering of Some Halo Nuclei of Proton at Energies Below 200 MeV/N

A.A. Ebrahim, S.R. Mokhtar, and Nagwa A. Ali*

Physics Department, Faculty of Science, Assiut University, Assiut 71516, Egypt

nagwa_physics1987@yahoo.com

ARTICLE INFO
Article History:
Received: 2023-05-06
Accepted: 2023-05-29
Online: 2023-08-30

Keywords:
Optical potential
São-Paulo potential
Proton elastic scattering
Halo nuclei

ABSTRACT

A microscopic approach was used to analyse the investigation of the elastic scattering of protons on ^{4,6,8}He at energies up to 200 MeV/N. The microscopic single folding (SF) and São-Paulo (SP) potentials were used to generate the real part of the optical model potential, and the Woods-Saxon form was used to phenomenologically compute the imaginary part. Three distinct nuclear densities (GG, GO, and G2S) of ^{4,6,8}He and Gaussian form effective NN interactions were used to determine the SF potential. A renormalization factor N_R of the folded real potential as well as the imaginary and spin-orbit potentials were among the free parameters used in the investigation, which was carried out using the FRESCO code. In addition, the overall reaction cross-sections σ_R in the three densities (GG, GO, and G2S) and the related real and imaginary volume integrals of interacting nucleon pairs were examined. The differential and reaction cross-section values that were obtained were in fair accord with the experimental data.

1.INTRODUCTION

The elastic scattering of protons from light nuclei may be studied using phenomenological and microscopic optical models at a variety of incidental energies [1-4]. Despite the fact that the phenomenological OP provides a simple analytic formulation (by utilizing the Woods-Saxon form), explicitly parameterized by the depth, radius, and diffuseness, it suffers one of the well-known flaws involving two sorts of "parameter ambiguities" discrete and continuous. The nucleus-nucleus interaction potential is calculated using a variety of techniques, including the folding model. Over the past several decades, simulations based on the folding model have been utilized to examine scattering mechanisms for numerous interacting systems utilizing microscopic and semi-microscopic methods.

The most effective use of a radioactive nuclear beam was the discovery of the unusual structure of nuclei close to drip lines. Weak binding energies that result in abnormally unusual characteristics describe these halo nuclei. A specific slope of the density distribution greater than the typical spatial extent distinguishes the halo nucleus. The enhanced interaction cross-section, comparable to those of its neighboring stable isotopes, serves as evidence. It is described as a core plus one or two neutrons. Also, the average nucleon separation energy in stable nuclei is about 6-8 MeV, while the separation energy of the halo neutron is very low, in some cases less than 1 MeV, see Table 1. Typical examples of halo neutron isotopes are helium (^{6,8}He), lithium (^{11}Li), beryllium (^{14}Be), and others, in which several neutrons are positioned in the far-extended nuclear periphery, to study the structure of exotic nuclei and analyze their elastic scattering on protons or nuclear targets at different energies. There are many experiments on the scattering of helium isotopes on protons at incident energies E_{lab} less than 100 MeV/N, namely for ^{6}He at energy 25.2[5-8], 38.3 [9],41.6 [10-12] and 71 MeV/N [13, 14] for ^{8}He at energy 15.7 [15], 25.2 [8], 32 [13, 14], 66 [10, 11] and 73 MeV/N [16].

Table 1: The half-life time and the separation energies of the halo nucleon(s) for some nuclei.

Candidates	*Valence nucleons*	*Separation energy MeV[17]*	*Half-life T1/2 ms[17]*

^{6}He	2n	0.972	806.7
^{8}He	4n	3.10	119.0

At energies up to 200 MeV/N, Maridi [18] computed the proton elastic scattering of various light-stable and halo nuclei, such as ^{4,6,8}He, using optical potentials and some fitting parameters from the microscopic OP. Additionally, Korsheninnikov et al. [13, 14] have examined the proton elastic scattering of ^{4,6,8}He and ^{7,9,11}Li at energies between 60 and 75 MeV/nucleon. Given that ^{6,8}He and ^{6}Li have radii of matter greater than that of the particle, it is discovered that the elastic scattering of these particles at low energies is comparable to and essentially different from that of ^{4}He. The scattering is further dependent on the matter radius of these nuclei. Additionally, Lukyanov et al.[19] compute the optical potentials and cross-sections of p+^{6}He elastic scattering at three distinct energies: E = 25.2, 41.6, and 71 MeV/N. Using simply the free parameters (N_R and N_I), which renormalize the depths of the real and imaginary sections of the OP, the OP's may be microscopically estimated inside the real part (V_F) and calculated within the HEA imaginary component (W_H). As a result, it is not essential to include many fitting parameters, and their method may be used with systems whose energies are less than 100 MeV/N.

The SF model is considered by utilizing parameterized nucleon-nucleon interaction folded with the target density. Also, it can be calculated by folding a nucleon-target optical potential folded with the projectile density[16]. Phenomenological analysis of the nucleon-nucleus interaction through the optical model is also considered to be an important intermediate step toward a full microscopic understanding of this interaction. The analysis of the experimental data is performed in the nucleon-nucleus interaction by obtaining the real part of the folding procedure V(r) and using Woods-Saxon (WS) or derivative Woods-Saxon forms for the imaginary parts of the potential[20, 21] , as well as spin-orbit potential which is introduced due to the 0.5 spin of protons.

The potential of São Paulo (SP) is a heavy-ion nuclear interaction theoretical model. It successfully describes the elastic, inelastic scattering, transfer, and fusion processes for heavy-ion reactions[22]. The proton-nucleus interaction is used as a well-known tool for probing the ground state density of the interacting nucleus since the interaction potential can be related to this density [23].

The present work focused on: firstly, reanalyzing elastic scattering data for p+^{4,6,8}He nuclear system at energies up to 200 MeV/nucleon using a microscopic method within the framework of single folding (SF) and São-Paulo (SP) potential. Secondly, it investigates the energy dependence of the reaction cross-sections and the volume integrals of the considered reactions. The real part of the optical potential OP is calculated microscopically using a realistic, effective nucleon-nucleon (NN) interaction folded with the nuclear matter density distribution of the target. The imaginary potential is taken in Woods-Saxon form to generate the required optical potential for analyzing the experimental data at incident energies listed in Table 2. The differential cross-section is reasonably well reproduced at forward angles. Our calculations have been obtained by taking different matter density distributions for ^{4,6,8}He as inputs in both potentials. They have the forms that are labeled as Gaussian-Gaussian (GG) ρGG, Gaussian-Oscillator (GO) ρGO, and Gaussian-2s (G2S) $\rho G2s$ [16]. To give the best fit to the experimental data, a renormalization of the folding potential is required to attenuate the uncertainties in the parameters. N_R is a normalization factor for the real potential. The outcomes are compared with each other as well as the experimental data. The manuscript is organized as follows: in the next section the theoretical formalism is presented, while the Results and discussion are shown in sect. 3, and conclusions are summarized in sect. 4.

Table 2: dσ/dΩ data of helium isotopes on proton elastic scattering.

Data	***Nuclear reaction***	***energy (MeV/N) [Ref.]***
dσ/d**Ω**	p+^{4}He	12.04, 17.45 [24], 31.0 [25], 40 [26], 52.3, 64.9 [27], 71.9 [28], 85 [29], and 156 [30]

^{6}He+p	25.1 [31-33], 38.3 [9],40.9 [11],41.6 [10, 12], and 71[13, 14, 34, 35]
^{8}He+p	15.7[36], 26.1 [37], 32 [38], 66[39], and 72 [16, 40]

2.THEORETICAL FORMALISM

2.1 Density distribution

The proton and neutron density distributions in the target nuclei are the most crucial inputs needed to calculate the nucleon-nucleus optical potential. The neutron-rich nucleus is treated by writing the neutron density distribution as [41, 42]:

$$\rho(r) = N_{co}\rho_{co}(r) + N_{va}\rho_{va}(r) \qquad (1)$$

Where the distributions of the core and valence nucleons are denoted by ρ_{co} and ρ_{va}, respectively. Also, N_{co} is the number of nucleons in the core and N_{va} is the number of neutrons in the halo part. In general, the study assumes that the core part in the target matter density has the Gaussian form

$$\rho_{co}(r) = \frac{1}{\pi^{1.5}{a_{co}}^3} e^{-r^2/{a_{co}}^2} \qquad (2)$$

Where $a_{co} = \sqrt{2/3}\, R_{co}$ is the diffuseness parameter of the core, where, R_{co} is the root main square (rms) radius of the core part. For the tail part (valence), the matter density has two different forms. The first ${\rho_{va}}^{G}(r)$ describes the Gaussian distribution [43-45]

$${\rho_{va}}^{G}(r) = \frac{1}{\pi^{1.5}{a_G}^3} e^{-r^2/{a_G}^2}, \qquad (3)$$

Where $a_G = \sqrt{2/3}\, R_{va}$ is the diffuseness parameter of the halo partition while R_{va} is the rms radius of the halo part. The radii R_{co} and R_{va} relate to the matter radius of the neutron halo nucleus R_m by the relation

$$R_m = \sqrt{\frac{N_{co}{R_{co}}^2 + N_{va}{R_{va}}^2}{A_P}} \qquad (4)$$

A 1p-shell harmonic oscillator density is used for the second one. This density manifests as [43, 44]:

$$\rho_{va}{}^{o}(r) = \frac{1}{1.5\pi^{1.5}a_o{}^5} r^2 e^{-r^2/a_o{}^2} \quad (5)$$

Where $a_o = \sqrt{2/5}\ R_{va}$ is the diffuseness parameter of the halo partition.

The last form is supposed that the valence neutrons are in 2s-state [13, 46] and it takes the form:

$$\rho_{va}{}^{2s}(r) = \frac{1}{1.5\pi^{1.5}a_{2s}{}^8}\left(\frac{r^2}{a_{2s}{}^2} - \frac{3}{2}\right)e^{-r^2/a_{2s}{}^2} \quad (6)$$

Where $a_{2s} = \sqrt{2/7}\ R_v$

The examined nuclei's density parameters, together with the relevant references and their configurations, are mentioned in Table 3.

Table 3:Root-mean-square radii of core and valence nucleons that used for the densities of the considered exotic nuclei.

Nucleus	*configuration*	*Rc (fm)*	*Rv (fm)*	*Rm(fm)*	*Ref.*
^{4}He	^{4}He	1.49	—	1.49	[47]
^{6}He	^{4}He+2n	1.72	3.23	2.33	[48]
^{8}He	^{4}He+4n	1.75	3.05	2.49	[48]

The ^{4,6,8}He densities are shown in Fig.1A, and B (GG, GO, and G2S) density distributions of ^{6}He (as the core of the ^{6}He nucleus) have long tails that clearly show their halo structure with large radii greater than the ^{4}He density. The density is demonstrated to be essentially produced from the core at r < 6 fm. However, the halo contribution predominates at r > 7 fm. Compared to the density distribution of the ^{4}He nucleus, the density distribution of the ^{6}He nucleus has an odd long tail[42]. The G2S density clearly shows a change in slope in the density distribution herewith describing the halo nature of the nucleus. This change is less manifest in Gaussian formalism (GO). Fig.1B represents

the nuclear density of the ^{8}He isotope, which also has extended tails compared with the ^{4}He density, which is treated as a core of ^{8}He nucleus but with less radius than ^{6}He.

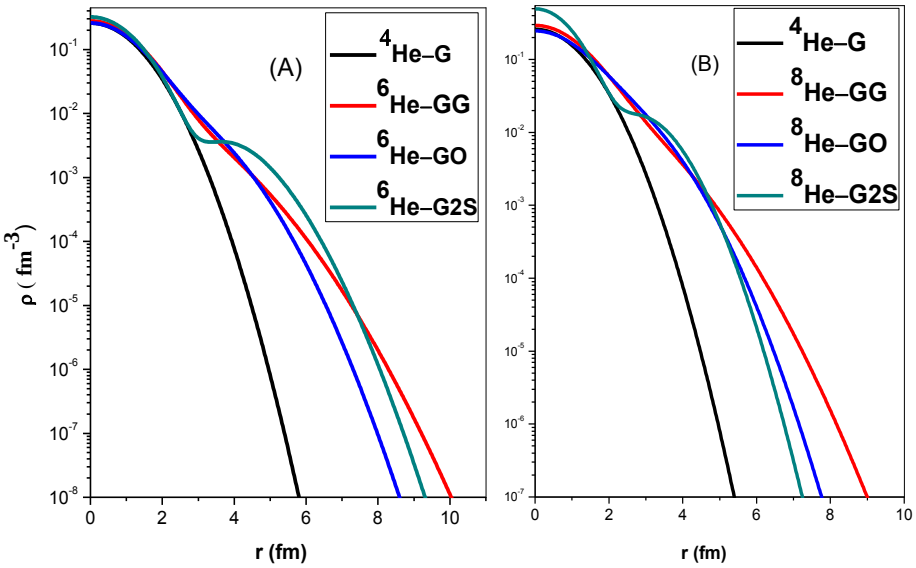

Fig 1. The halo neutron density distribution with Gaussian (ρ^{GG}) ***(red line), harmonic oscillator*** (ρ^{GO}) ***(blue line), (dark cyan)*** (ρ^{G2S}) ***densities and (black line) for the core nucleus. Figs1A, and B represent the nuclear densities of helium isotopes.***

2.2 Nucleon-Nucleon Interaction

2.2.1 Single folding optical potential (SFOP) model

Greenlees et al. [49] acquire the folding model in a variational calculation to represent nucleon-nucleus elastic scattering data[50]. The phenomenological approach is usually very simple and successful in replicating the experimental angular distribution data. One of the well-known flaws of the optical model (OM) is "parameter ambiguities" such as discrete and continuous ambiguities. The SF potential is applied in the nucleon-nucleus scattering, which folds the density distributions of the projectile and target nuclei

with nucleon-nucleon interaction potential (v_{nn}). The proton is considered a projectile, as well the single folding potential is produced using Fortran and DOLFIN code [51, 52]. The SF potential is given by:

$$V_F(R) = \int \rho(r_1) v_{nn}(r_{12}) \; d\vec{r}_1 \qquad (7)$$

Where r_{12} refers to the projectile-target relative position vector, $\rho_1(r_1)$ is the density distribution for the target, and $v_{nn}(r_{12})$ is the effective nucleon-nucleon interaction.

In the case of the single folding v_{nn} (r_{12}) it is taken as a Gaussian form:

$$v_{nn}(r_{12}) = -v_0 \; e^{-k r_{12}^2}, \quad (\text{k = 0.46 fm-2, } v_0 = 22.332 \text{ MeV}) \qquad (8)$$

With the use of automated searching FRESCO, optical model analysis of elastic scattering are carried out. The whole potential appears as

$$U(R) = N_r V_F(R) + iW_i(R) \qquad (9)$$

The folding potential generated by Eq. (7) is used to represent the volume part of the real optical potential. The phenomenological Woods-Saxon (WS) shape is used to represent the imaginary portion of the optical potential and has the following form:

$$W_i(R) = -W_0 / [1 + exp\left(\frac{R - r_I}{a_I}\right)] \qquad (10)$$

Where $r_I = r_0 \, A_T^{1/3}$, W_0, r_0, and a_I are the depth, radius, and diffuseness parameters, respectively.

2.2.2 The São-Paulo potential (SP)

For numerous heavy ion systems across a very broad energy range, the So Paulo (SP) potential is successful in modeling the elastic scattering and peripheral reaction channels. The folding potential and nuclear interaction are linked by

$$V_N(R, E) = V_{FP}(R) \; e^{-4v^2/c^2} \qquad (11)$$

Where c is the speed of light, R is the separation distance between the centers of target and projectile nuclei, v is the local relative velocity between the two nuclei:

$$v^2(R,E) = \frac{2}{\mu}[E - V_c(R) - V_N(E,R)] \quad (12)$$

The target nucleus's charge distribution yielded the Coulomb potential, or V_c . It has a radius of RC. The Pauli non-locality's effects lead to the potential's velocity dependency[53, 54]. By iteratively resolving Eqs. (11 and 12), the SP potential is derived numerically. The folding potential depends on the matter densities of the nuclei involved in the collision is given by:

$$V_{FP}(R) = \int \rho(\vec{R})\, V_0\, \delta(\vec{R} - \vec{r})\; d\vec{r} \quad (13)$$

With V_0 = −456 MeV fm^3. The two distinct potentials of the OP as in Eqs. (7) and (11) are shown in Fig. 2, which shows the real potentials of the proton elastic scattering with helium nuclei in the energy range of 20 to 200 MeV/N. However, in ^{6}He at all densities, the two forms of the real OP are close together in the surface region. The depths of the optical potentials with various densities or interactions are varied at short distances, but they are fairly near to one another at the surface (at r > 5 fm). For ^{6}He at SF, the renormalized real potentials at small distances are shallower than those at SP, whereas ^{8}He has a deeper potential than ^{6}He and ^{4}He.

The search for the normalization factors ($N_r, N_I,$ and N_s) begins with a selection of N_r= 0.5-1.2, N_I=0.5-0.8 and N_s=0.5-0.8. The fitting process takes place to get a minimum χ^2. Where the χ^2 is given by[55]:

$$\chi^2 = \frac{1}{N}\sum_{j=1}^{N}\left[\frac{\sigma_{th}(\theta_j) - \sigma_{exp}(\theta_j)}{\Delta\sigma_{exp}(\theta_j)}\right]^2 \quad (14)$$

Where the cross-sections at the angle θ_j are determined theoretically and experimentally by $\sigma_{th}(\theta_j)$ and $\sigma_{exp}(\theta_j)$, respectively. N is the number of data points, and $\Delta\sigma_{exp}(\theta_j)$ is the experimental error.

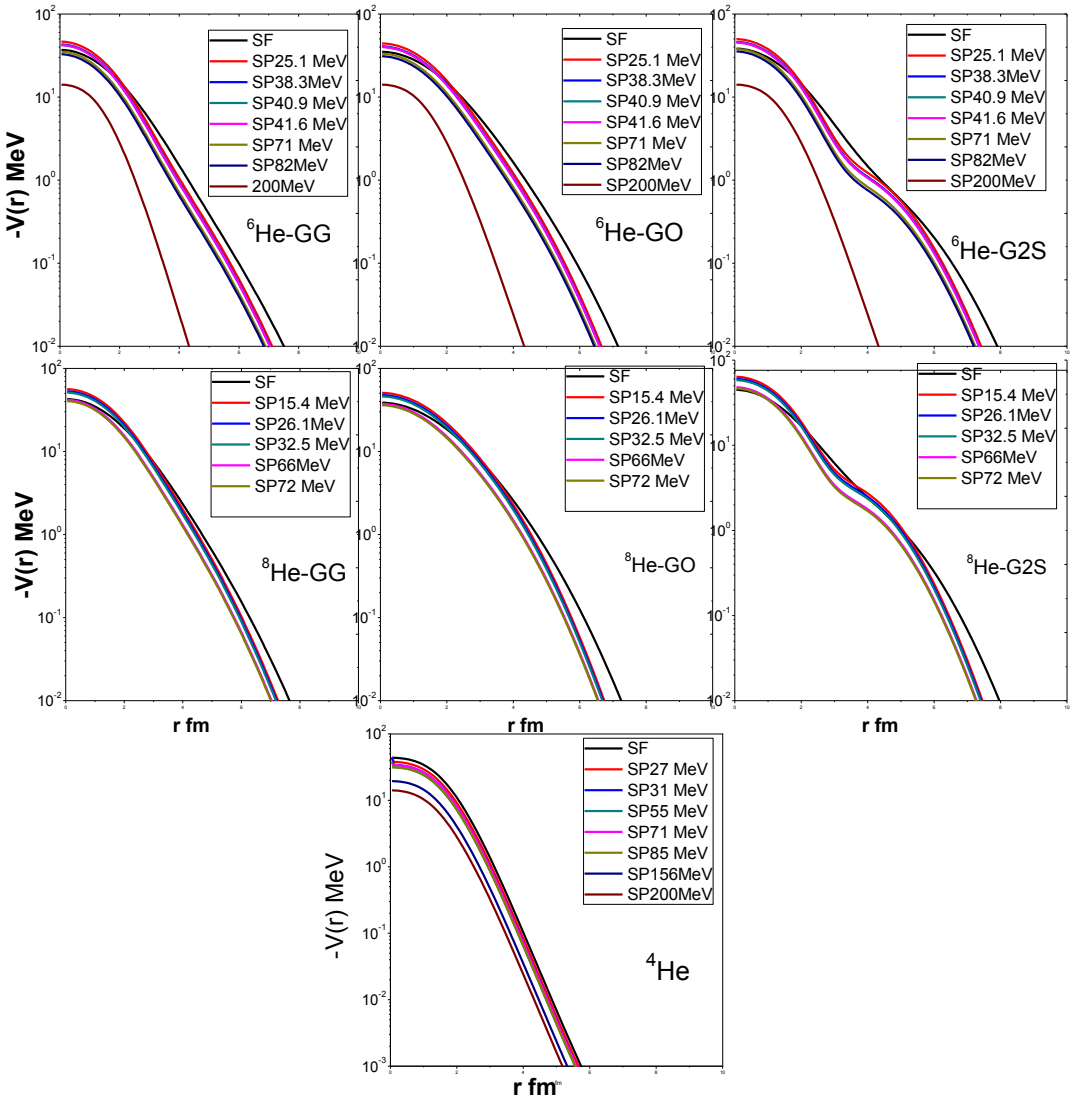

Fig 2: Real optical potentials for helium isotopes elastic scattering of proton.

RESULTS

Calculations for the proton elastic scattering of some helium nuclei, especially ^{4,6,8}He at energies up to 200 MeV/N, were done using the optical model potentials [Eq. (9)].

The SF potential was derived using [Eq. (7)] using three different nuclear densities of ^{4,6,8}He and Gaussian form effective NN interactions. The calculated potential, supplemented by phenomenological imaginary defined by [Eq. (10)], was used to

calculate the angular distributions of the P+^{4,6,8}He elastic scattering cross-section. The search is performed using FRESCO code on some free parameters; some of them are the imaginary and spin–orbit potentials, as well as a normalization factor N_R of the real folded potential.

The theoretical results were compared with the available experimental data within the framework of the SF model for P+^{4,6,8}He were calculated at energies that set before using microscopic SF and SP potentials where imaginary parts of the potential represented as wood-Saxon were shown in Fig 3, Fig 4 and Fig 5 respectively. It was noted from Fig 3 that the resulting angular distributions of the elastic scattering differential cross section produce for ^{4}He at G density are very good fit at energies 27.88, 31, 55, 71, 156, and 200 MeV with the experimental data; except for at energy 85 MeV there was a small diffraction 70^o angle, however, the results show that the two kinds of potentials precisely replicate the results of the experiment. The differential cross sections of ^{6,8}He proton elastic scattering at various energies (in MeV/nucleon) at GG, GO, and G2S densities are shown in Figs. 4 and 5. These cross-sections showed a satisfactory match throughout the whole observed angular range for low energies and intermediate energies in the two halo nuclei ^{6,8}He.

The real J_R and the imaginary volume integrals J_I deduced for ^{4,6,8}He off proton elastic scattering system using the SF and SP potentials. The behavior of the energy dependence of J_R, J_I and σ_R was shown from Fig.6 to Fig. 8. It is obvious that the resulting J_I values revealed clear energy dependence where J_I increased with increasing energy. Where J_R decreases with increasing energy but it was constantly in some Figs. According to Eqs (15,16) the volume integrals of the real and imaginary potentials are particularly dependent on their normalization factors (NR).

$$J_R = -\frac{4\pi}{A}\int [N_R\, V_F(R)]\, R^2\, dR, \qquad (15)$$

$$J_I = -\frac{4\pi}{A}\int \left[-W_v\, f_v(R) + 4\, a_s\, W_s \frac{d}{dr}\, f_s(R)\right] R^2\, dR \qquad (16)$$

Fig. 6 had the normal behavior of J_R and J_I for ^{4}He in the two potentials. Also, Figs.7 and 8 represented the J_R and J_I for ^{6}He and ^{8}He respectively. J_R decreased while J_I increased or steadied sometimes up to the same reasons reminded before. The dependency of the reaction cross-section on the energy for proton elastic scattering of ^{4}He was presented in

Fig.9. It was noted that the value of the reaction cross section σ_R sharply increased with increasing energy and then decreased at relatively higher energies. The same case at Figs. 10 and 11 where the reaction cross section σ_R for P+ ^{6}He and P+ ^{8}He respectively. They increased with increasing energy at low energies (~ 20 MeV/nucleon) reached almost a saturation value at relative intermediate energies then decreased. This is related to the scattered nuclei's rms radius.

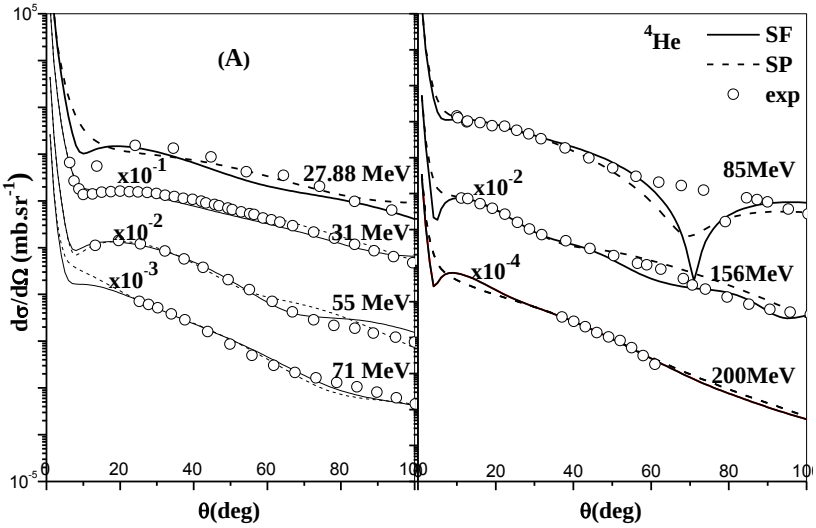

Fig 3: Differential cross sections of proton elastic scattering of ^{4}He at some energies (in MeV/N). The solid and dashed lines with SF and SP potentials represent the results of their calculations.

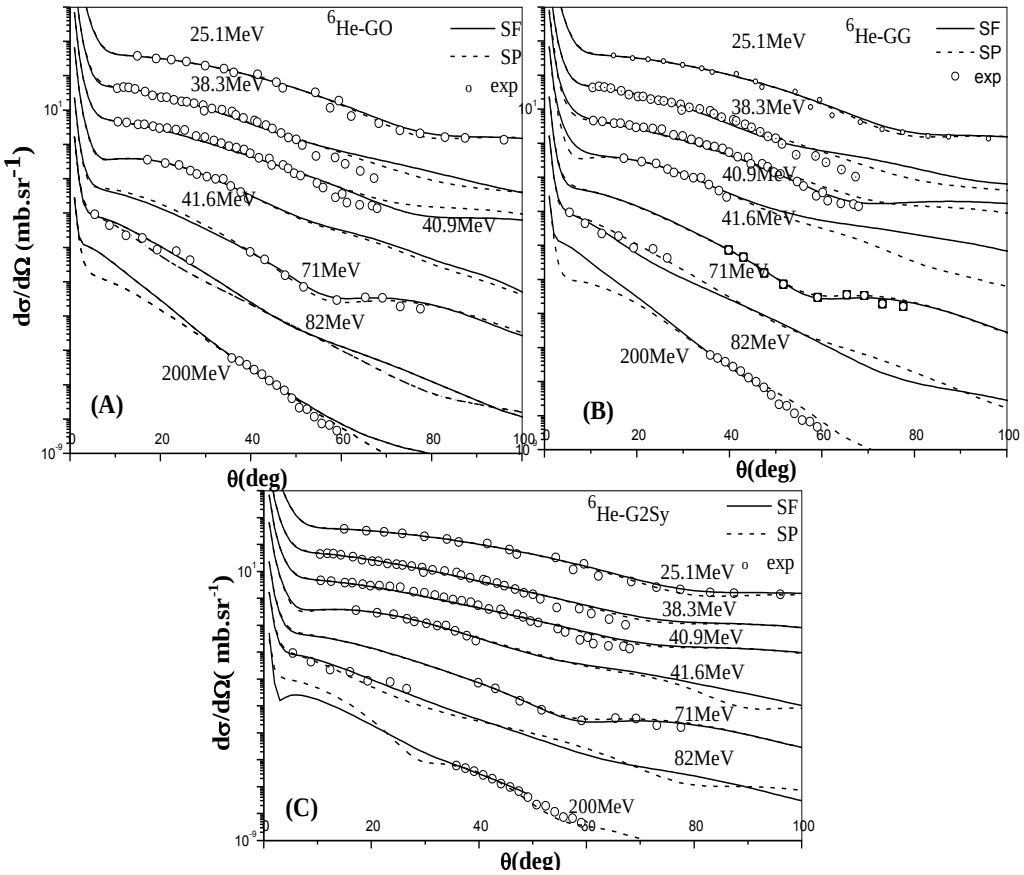

Fig 4: Differential cross sections of proton elastic scattering of ^{6}He at some energies (in MeV/N). The solid and dashed lines with SF and SP potentials represent the results of their calculations.

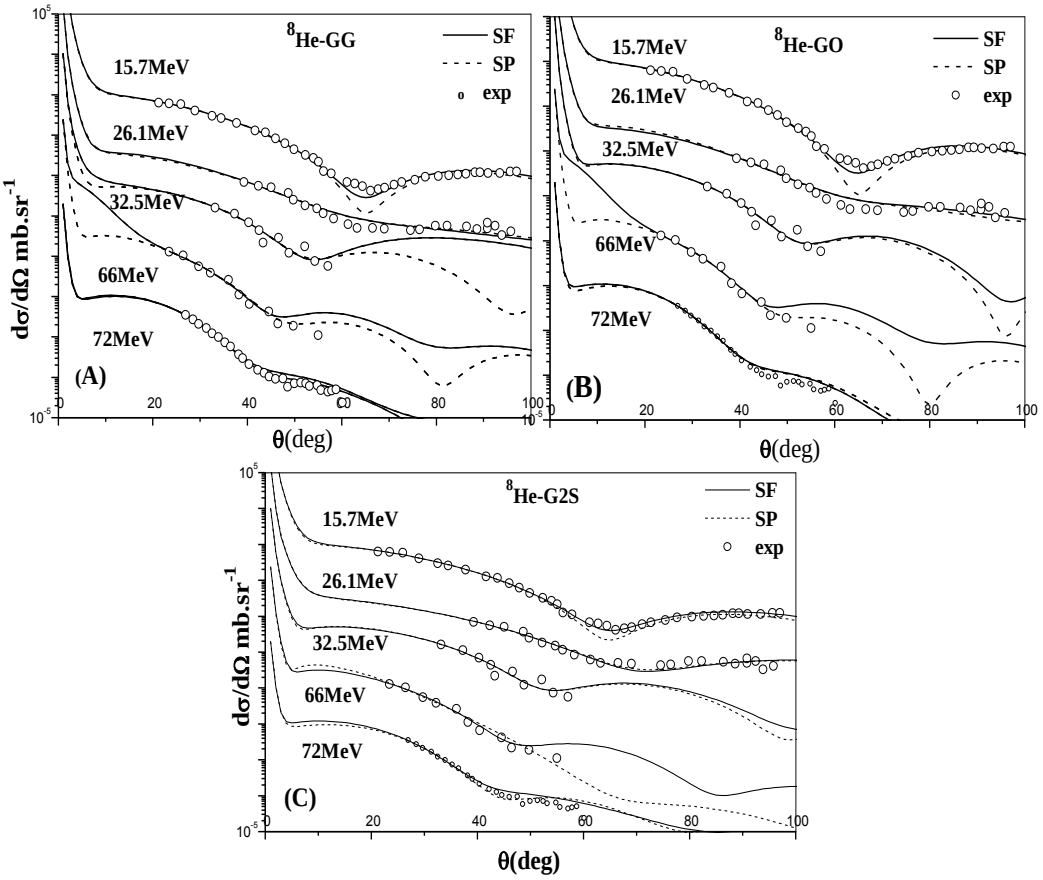

Fig 5: Differential cross sections of proton elastic scattering of ^{8}He at some energies (in MeV/N). The solid and dashed lines with SF and SP potentials represent the results of their calculations.

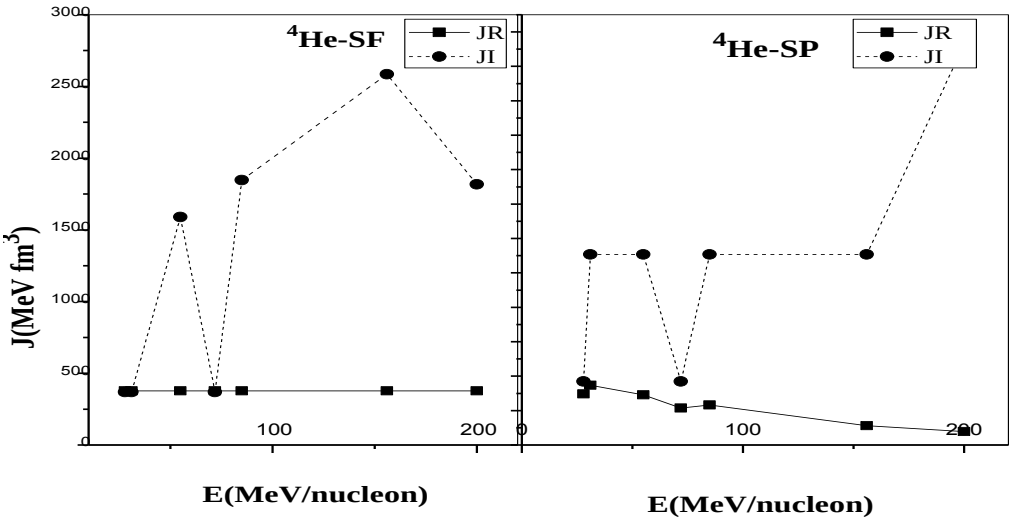

Fig 6: The volume integrals of P+ ^{4}He.

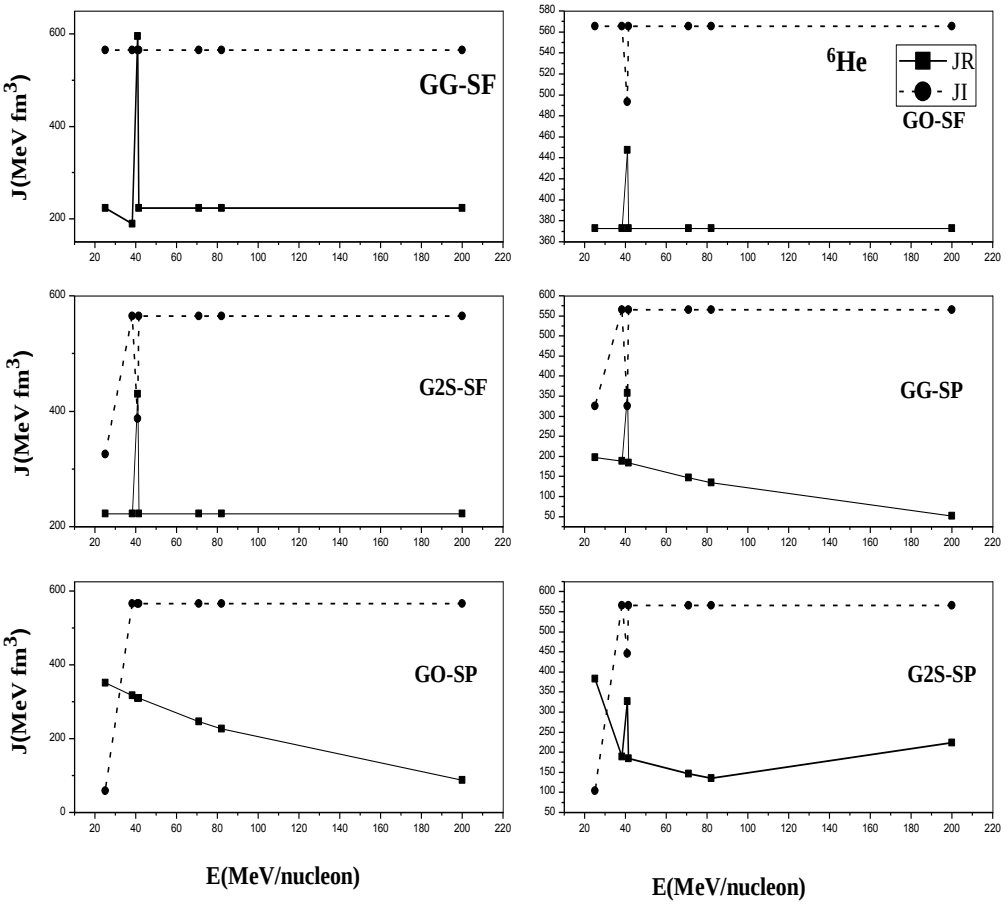

Fig 7: The volume integrals of ^{6}He+P at GG, GO and G2S density distributions.

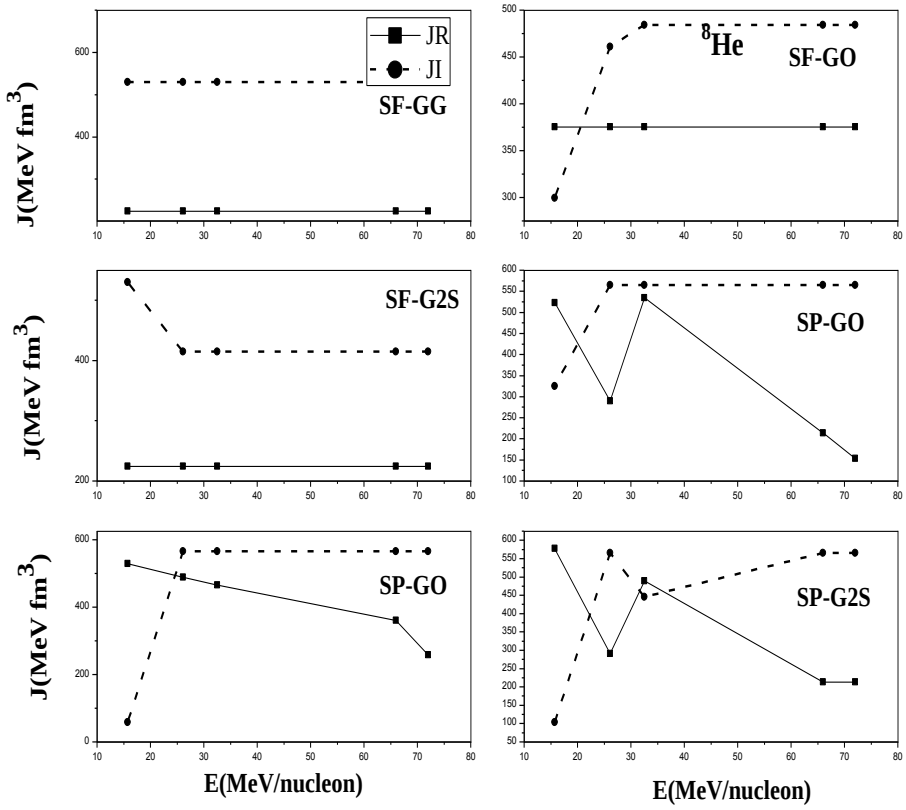

Fig 8: The volume integrals of ^{8}He+P at GG, GO and G2S density distributions

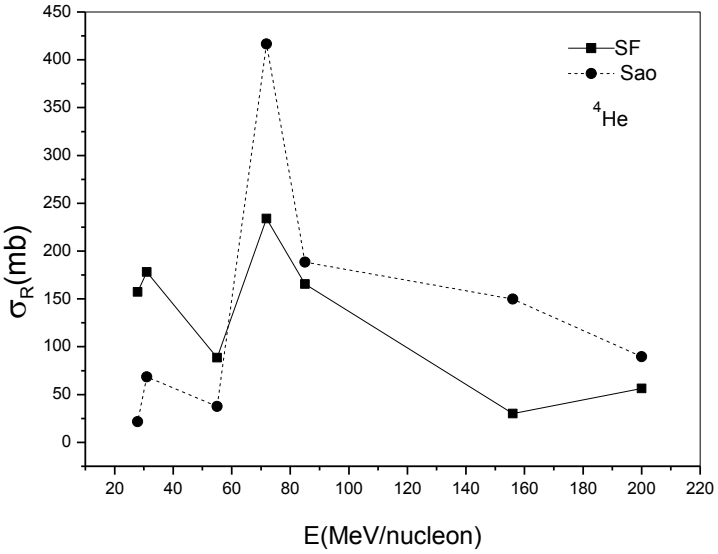

Fig 9: The reaction cross section σ_R of P+ ^{4}He.

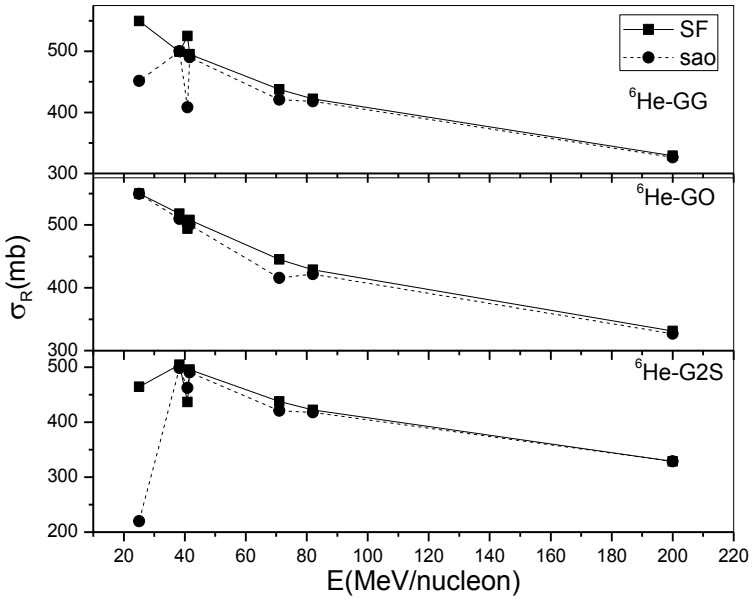

Fig 10: The reaction cross section σ_R of ^{6}He+ P.

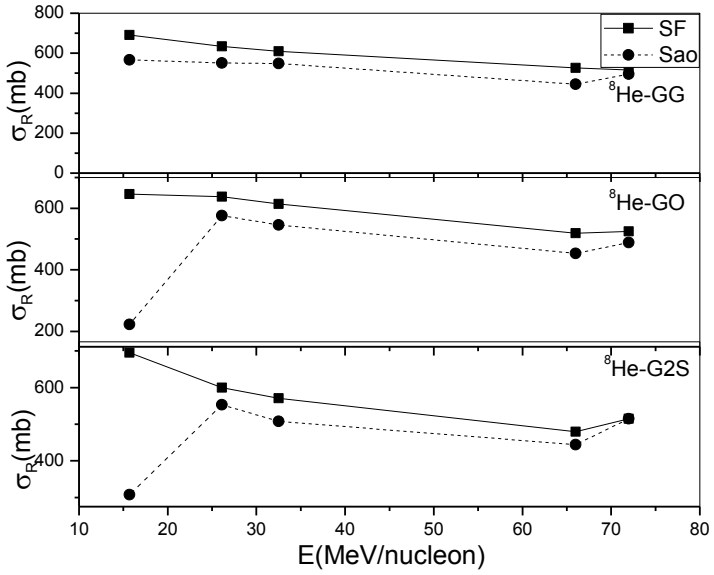

Fig 11: The reaction cross section σ_R of ^{8}He+ P.

CONCLUSION

The proton elastic scattering of some halo nuclei, such as ^{4,6,8}He at energies up to 200 MeV/nucleon using the optical model potentials is studied. The real part is constructed only from the single folding (SF) and São-Paulo (SP) potentials, the phenomenological imaginary part with Woods-Saxon form is used. The SF potential is derived considering three different nuclear densities of ^{4,6,8}He (GG, GO and G2S) and Gaussian form effective NN interactions. The ^{6,8}He densities are considered to be superimposed of two parts, a density for a core plus a density of two neutron halos. Where, the different distributions, in GG, GO and G2S density distributions of ^{6}He have extensive tails apparent in their halo structure with large radii which are larger than the ^{4}He density (which is a core of ^{6}He nucleus). The density of ^{8}He has also extended tails compared with the ^{4}He density, thus considered as a core of ^{8}He nucleus but with less radius than ^{6}He.

The real optical potentials of the proton elastic scattering with helium nuclei in a variety of energy ranges with the two different types of OP are provided, and it is determined that the potential of ^{8}He is deeper than that of ^{6}He and ^{4}He. On a few free parameters, including the imaginary and spin-orbit potentials as well as a normalisation factor N_R of the real folded potential, the search is carried out using the FRESCO code.

The overall reaction cross sections σR in the three densities (GG, GO, and G2S) and the associated real and imaginary volume integrals per interacting nucleon pair (JR and JI) in MeV fm^3 are shown. With the exception of the energy 85 MeV, where there is a little amount of diffraction at a 70^o angle, the resultant angular distributions of the elastic scattering differential cross section yield for ^{4}He at G density, extremely excellent fits to the experimental data for energies of 27,88, 31, 55, 71, 156, and 200 MeV. The findings showed that both potential types accurately reflect the experimental data; however, for most energies, SP offers a somewhat better match than SF. The differential cross sections of ^{6,8}He proton elastic scattering at various energies (in MeV/N) at the GG, GO, and G2S densities showed a satisfactory fitting throughout the whole observed angular range for

low and intermediate energy in the two halo nuclei. Therefore, the choice of density has some influence on how the differential cross-sections behave.

REFERENCES

[1] J. Holt, N. Kaiser, and G. Miller, "Microscopic optical potential for exotic isotopes from chiral effective field theory," Physical Review C, vol. 93, p. 064603, 2016.
[2] M. Farag, E. Esmael, and H. Maridi, "Energy-dependent microscopic optical potential for scattering of nucleons on light nuclei," The European Physical Journal A, vol. 50, pp. 1-10, 2014.
[3] M. Avrigeanu, W. Von Oertzen, A. Plompen, and V. Avrigeanu, "Optical model potentials for α-particles scattering around the Coulomb barrier on A∼ 100 nuclei," Nuclear Physics A, vol. 723, pp. 104-126, 2003.
[4] M. Avrigeanu, W. von Oertzen, F. Roman, and V. Avrigeanu, "Optical Model Potentials for α-Particles Scattering around the Coulomb Barrier on Medium-Mass Nuclei," in AIP Conference Proceedings, 2005, pp. 1116-1119.
[5] K. Rusek, K. Kemper, and R. Wolski, "6 He interaction with protons," Physical Review C, vol. 64, p. 044602, 2001.
[6] L. Giot, P. Roussel-Chomaz, S. Pita, N. Alamanos, F. Auger, M.-D. Cortina-Gil, et al., "Search for t+ t clustering in 6He," Nuclear Physics A, vol. 738, pp. 426-430, 2004.
[7] K. Lukyanov, V. Lukyanov, E. Zemlyanaya, A. Antonov, and M. Gaidarov, "Calculations of 6 He+ p elastic-scattering cross-sections using folding approach and high-energy approximation for the optical potential," The European Physical Journal A, vol. 33, pp. 389-400, 2007.
[8] G. Ter-Akopian and W. Greiner, "Fundamental issues in elementary," in Proceedings of the Symposium in honor and memory of Michael Danos, Bad Honnef, Germany, 2000, p. 371.
[9] V. Lapoux, N. Alamanos, F. Auger, Y. Blumenfeld, J.-M. Casandjian, M. Chartier, et al., "Coupling effects in the elastic scattering of the exotic nucleus 6He on protons," Physics Letters B, vol. 517, pp. 18-24, 2001.
[10] M. Cortina-Gil, P. Roussel-Chomaz, N. Alamanos, J. Barrette, W. Mittig, F. Auger, et al., "Elastic scattering and charge exchange reaction with light neutron rich exotic beams," Nuclear Physics A, vol. 616, pp. 215-222, 1997.
[11] A. Lagoyannis, F. Auger, A. Musumarra, N. Alamanos, E. Pollacco, A. Pakou, et al., "Probing the 6He halo structure with elastic and inelastic proton scattering," Physics Letters B, vol. 518, pp. 27-33, 2001.
[12] M. Cortina-Gil, P. Roussel-Chomaz, N. Alamanos, J. Barrette, W. Mittig, F. Auger, et al., "Search for the Signature of a Halo Structure in the p (6He, 6Li) n Reaction," Physics Letters B, vol. 371, pp. 14-18, 1996.
[13] A. Korsheninnikov, E. Kuzmin, E. Y. Nikolskii, C. Bertulani, O. Bochkarev, S. Fukuda, et al., "Elastic and inelastic scattering of exotic nuclei," Nuclear Physics A, vol. 616, pp. 189-200, 1997.
[14] A. A. Korsheninnikov, E. Y. Nikolskii, C. Bertulani, S. Fukuda, T. Kobayashi, E. Kuzmin, et al., "Scattering of radioactive nuclei 6He and 3H by protons: Effects of neutron skin and halo in 6He, 8He, and 11Li," Nuclear Physics A, vol. 617, pp. 45-56,

1997.
[15] F. Skaza, N. Keeley, V. Lapoux, N. Alamanos, F. Auger, D. Beaumel, et al., "Important pickup coupling effect on He8 (p, p) elastic scattering," Physics Letters B, vol. 619, pp. 82-87, 2005.
[16] A. Korsheninnikov, K. Yoshida, D. Aleksandrov, N. Aoi, Y. Doki, N. Inabe, et al., "Experimental study of 8He+ p elastic and inelastic scattering," Physics Letters B, vol. 316, pp. 38-44, 1993.
[17] G. Audi, A. Wapstra, and C. Thibault, "The AME2003 atomic mass evaluation:(II). Tables, graphs and references," Nuclear physics A, vol. 729, pp. 337-676, 2003.
[18] M. Farag, E. Esmael, and H. Maridi, "Elastic interaction of protons with stable and exotic light nuclei," Physical Review C, vol. 88, p. 064602, 2013.
[19] K. Lukyanov, V. Lukyanov, E. Zemlyanaya, A. Antonov, and M. Gaidarov, "Calculations of 6 He+ p elastic-scattering cross-sections using folding approach and high-energy approximation for the optical potential," The European Physical Journal A, vol. 33, pp. 389-400, 2007.
[20] F. Brieva and J. Rook, "Nucleon-nucleus optical model potential:(ii). finite nuclei," Nuclear Physics A, vol. 291, pp. 317-341, 1977.
[21] M. Mehta and S. Kailas, "Proton-nucleus optical model potential at low energies—a review," Pramana, vol. 27, pp. 139-160, 1986.
[22] L. Gasques, L. C. Chamon, D. Pereira, M. Alvarez, E. Rossi Jr, C. P. Silva, et al., "Global and consistent analysis of the heavy-ion elastic scattering and fusion processes," Physical Review C, vol. 69, p. 034603, 2004.
[23] C. A. Bertulani and H. Sagawa, "Probing the ground-state and transition densities of halo nuclei," Nuclear Physics A, vol. 588, pp. 667-692, 1995.
[24] D. Garreta, J. Sura, and A. Tarrats, "Differential cross section and polarization in p-α scattering at 12, 14.2 and 17.5 MeV," Nuclear Physics A, vol. 132, pp. 204-212, 1969.
[25] S. Bunch, H. Forster, and C. Kim, "Interactions of 31 MeV protons with He4," Nuclear Physics, vol. 53, pp. 241-251, 1964.
[26] M. K. Brussel and J. H. Williams, "Elastic Scattering of 40-Mev Protons by He 4," Physical Review, vol. 106, p. 286, 1957.
[27] K. Imai, K. Hatanaka, H. Shimizu, N. Tamura, K. Egawa, K. Nisimura, et al., "Polarization and cross section measurements for p-4He elastic scattering at 45, 52, 60 and 65 MeV," Nuclear Physics A, vol. 325, pp. 397-407, 1979.
[28] S. Burzynski, J. Campbell, M. Hammans, R. Henneck, W. Lorenzon, M. Pickar, et al., "p− 4 He scattering: New data and a phase-shift analysis between 30 and 72 MeV," Physical Review C, vol. 39, p. 56, 1989.
[29] L. Votta, P. Roos, N. Chant, and R. Woody III, "Elastic proton scattering from $ sup 3$ He and $ sup 4$ He and the $ sup 4$ He (p, d) $ sup 3$ He reaction at 85 MeV," University of Maryland, College Park, Maryland 207421974.
[30] V. Comparat, R. Frascaria, N. Fujiwara, N. Marty, M. Morlet, P. Roos, et al., "Elastic proton scattering on He 4 at 156 MeV," Physical Review C, vol. 12, p. 251, 1975.
[31] R. Wolski, A. Fomichev, A. Rodin, S. Sidorchuk, S. Stepantsov, G. Ter-Akopian, et al., "Cluster structure of 6He studied by means of 6He+ p reaction at 25 MeV/n

energy," Physics Letters B, vol. 467, pp. 8-14, 1999.
[32] S. Stepantsov, D. Bogdanov, A. Fomichev, A. Rodin, S. Sidorchuk, R. Slepnev, et al., "24.5 A MeV 6He+ p elastic and inelastic scattering," Physics Letters B, vol. 542, pp. 35-42, 2002.
[33] L. Giot, P. Roussel-Chomaz, C. Demonchy, W. Mittig, H. Savajols, N. Alamanos, et al., "Investigation of He 6 cluster structures," Physical Review C, vol. 71, p. 064311, 2005.
[34] T. Uesaka, S. Sakaguchi, Y. Iseri, K. Amos, N. Aoi, Y. Hashimoto, et al., "Analyzing power for proton elastic scattering from the neutron-rich he 6 nucleus," Physical Review C, vol. 82, p. 021602, 2010.
[35] S. Sakaguchi, Y. Iseri, T. Uesaka, M. Tanifuji, K. Amos, N. Aoi, et al., "Analyzing power in elastic scattering of 6 He from a polarized proton target at 71 MeV/nucleon," Physical Review C, vol. 84, p. 024604, 2011.
[36] F. Skaza, V. Lapoux, N. Keeley, N. Alamanos, E. Pollacco, F. Auger, et al., "Experimental evidence for subshell closure in He 8 and indication of a resonant state in He 7 below 1 MeV," Physical Review C, vol. 73, p. 044301, 2006.
[37] R. Wolski, A. Fomichev, A. Rodin, S. Sidorchuk, S. Stepantsov, G. Ter-Akopian, et al., "Interaction of 8He nuclei with α particles and protons at a beam energy of 26 MeV/n," Nuclear Physics A, vol. 701, pp. 29-34, 2002.
[38] A. Korsheninnikov, E. Y. Nikolskii, T. Kobayashi, D. Aleksandrov, M. Fujimaki, H. Kumagai, et al., "Spectroscopy of 12Be and 13Be using a 12Be radioactive beam," Physics Letters B, vol. 343, pp. 53-58, 1995.
[39] A. Korsheninnikov, E. Y. Nikolskii, T. Kobayashi, A. Ozawa, S. Fukuda, E. Kuzmin, et al., "Spectroscopy of the halo nucleus Li 11 by an experimental study of Li 11+ p collisions," Physical Review C, vol. 53, p. R537, 1996.
[40] S. Sakaguchi, T. Uesaka, N. Aoi, Y. Ichikawa, K. Itoh, M. Itoh, et al., "Shallow and diffuse spin-orbit potential for proton elastic scattering from neutron-rich helium isotopes at 71 MeV/nucleon," Physical Review C, vol. 87, p. 021601, 2013.
[41] M. Sharma and W. Haider, "Study of 11Li+ p elastic scattering using BHF formalism with three body force," Journal of Physics G: Nuclear and Particle Physics, vol. 45, p. 045102, 2018.
[42] R. Kanungo and C. Samanta, "Halo structure of 11 Li in proton elastic scattering: a folding model description with isospin, density and momentum dependent effective interaction," in DAE symposium on nuclear physics: contributed papers. Volume 39B (1996), 1996.
[43] A. Dobrovolsky, G. Alkhazov, M. Andronenko, A. Bauchet, P. Egelhof, S. Fritz, et al., "Study of the nuclear matter distribution in neutron-rich Li isotopes," Nuclear Physics A, vol. 766, pp. 1-24, 2006.
[44] S. Ilieva, F. Aksouh, G. Alkhazov, L. Chulkov, A. Dobrovolsky, P. Egelhof, et al., "Nuclear-matter density distribution in the neutron-rich nuclei 12, 14Be from proton elastic scattering in inverse kinematics," Nuclear Physics A, vol. 875, pp. 8-28, 2012.
[45] M. Hassan, M. N. El-Din, A. Ellithi, H. Hosny, and T. Salama, "Sensitivity of the halo nuclei-12 C elastic scattering at incident nucleon energy 800 MeV to the halo density distribution," Indian Journal of Physics, vol. 91, pp. 1245-1258, 2017.
[46] M. Zhukov, B. Danilin, D. Fedorov, and J. Bang, "lJ Thompson and JS Vaagen," Phys. Rep, vol. 231, p. I31, 1993.

[47] G. Alkhazov, A. Dobrovolsky, P. Egelhof, H. Geissel, H. Irnich, A. Khanzadeev, et al., "Nuclear matter distributions in the 6He and 8He nuclei from differential cross sections for small-angle proton elastic scattering at intermediate energy," Nuclear Physics A, vol. 712, pp. 269-299, 2002.
[48] I. Tanihata, D. Hirata, T. Kobayashi, S. Shimoura, K. Sugimoto, and H. Toki, "Revelation of thick neutron skins in nuclei," Physics Letters B, vol. 289, pp. 261-266, 1992.
[49] G. Greenlees, G. Pyle, and Y. Tang, "Nuclear-matter radii from a reformulated optical model," Physical Review, vol. 171, p. 1115, 1968.
[50] A. Chaudhuri, "Density distribution of Li 11 and proton elastic scattering from Li 9 and Li 11," Physical Review C, vol. 49, p. 1603, 1994.
[51] S. Hamada, "Single Folding Optical Potential for Elastic Scattering of Protons from 14 N and 16 O in a Wide Range of Energies," Physics of Particles and Nuclei Letters, vol. 15, pp. 143-147, 2018.
[52] J. Cook, "DFPOT-a program for the calculation of double folded potentials," Computer Physics Communications, vol. 25, pp. 125-139, 1982.
[53] M. C. Ribeiro, L. C. Chamon, D. Pereira, M. Hussein, and D. Galetti, "Pauli nonlocality in heavy-ion rainbow scattering: A further test of the folding model," Physical review letters, vol. 78, p. 3270, 1997.
[54] L. C. Chamon, D. Pereira, M. S. Hussein, M. C. Ribeiro, and D. Galetti, "Nonlocal description of the nucleus-nucleus interaction," Physical review letters, vol. 79, p. 5218, 1997.
[55] G. R. Satchler and W. G. Love, "Folding model potentials from realistic interactions for heavy-ion scattering," Physics Reports, vol. 55, pp. 183-254, 1979.